

Spin crossover of the octahedral Co ion in Co₃S₄: Emergence of hidden magnetismInseo Kim,¹ Hyungwoo Lee,¹ Ho-Hyun Nahm², and Minseok Choi^{1,*}¹Department of Physics, Inha University, Incheon 22212, Republic of Korea²Department of Physics, Korea Advanced Institute of Science and Technology, Daejeon 34141, Republic of Korea

(Received 25 March 2022; revised 7 July 2022; accepted 17 August 2022; published 31 August 2022)

It is well established that the ground-state electron configuration of the octahedral Co³⁺ ion is $t_{2g}^6 e_g^0$, which corresponds to a low-spin (LS) state. However, we theoretically demonstrate that the octahedral Co³⁺ ion in Co₃S₄ prefers a high-spin (HS) state with the $t_{2g}^4 e_g^2$ configuration, resulting in unusual magnetism. The density-functional theory plus U calculation and ligand-field theory show that weak crystal-field splitting associated with S²⁻ induces a spin crossover from the LS to HS state of the octahedral Co³⁺ ion along with a weak Jahn-Teller-like elongation, and as a result, a ferromagnetic (FM) metal phase is energetically stabilized. Nevertheless, this phase is significantly more stable than the antiferromagnetic (AFM) phase experimentally reported at low temperature. Furthermore, phonon calculations suggest that the FM metal phase is possibly one of the Co₃S₄ polymorphs, appearing in the certain experimental growth environment, but it is not expected to appear due to a temperature-dependent transition from the AFM phase. In addition, the Lyons, Kaplan, Dwight, and Menyuk theory shows that this phase is further expected to undergo a phase transition to the frustrated magnetic state. We believe that our work provides insight into magnetism of cobalt compounds and also paves the way to achieve the HS Co³⁺ by design.

DOI: [10.1103/PhysRevResearch.4.033171](https://doi.org/10.1103/PhysRevResearch.4.033171)

I. INTRODUCTION

Spin crossover (SCO) phenomena, in which multiple spin states exhibit stability upon exposure to external stimuli such as temperature [1,2], are of great interest to researchers. The SCO behavior is potentially associated with smart materials and other promising materials that are suitable as components of memory devices, displays, sensors, and mechanical devices [2]. The octahedrally coordinated Co³⁺ ion with $3d^6$ electrons is an ideal platform for studying the SCO phenomena owing to the ambiguity of its spin state [3]. It is well established that the octahedral Co³⁺ ion prefers a low-spin (LS) state ($t_{2g}^6 e_g^0$, $S = 0$) at the ground state. However, electron transfer from the t_{2g} to e_g level by external stimuli is reasonably possible, allowing additional spin degrees of freedom, owing to a small difference (≤ 0.08 eV) between the crystal-field splitting energy Δ_o and Hund's coupling energy [4]. A typical example of an SCO material is LaCoO₃. The Co³⁺ ion in this material is positioned at the center of the oxygen octahedra, and it has been observed to be in the magnetic LS, high-spin (HS; $t_{2g}^4 e_g^2$, $S = 2$), intermediate-spin (IS; $t_{2g}^5 e_g^1$, $S = 1$), or LS-HS mixed-spin state [5–8].

This indicates that the stable HS/IS state of Co³⁺ ions can be achieved in SCO materials in a controllable manner. According to the ligand field theory, one can speculate that the anion sublattice in solids, comprising a weaker field ligand

than oxygen in the spectrochemical series, is likely to exhibit the HS/IS Co³⁺ ion. In other words, the ambiguity of the Co³⁺ spin state might be eliminated when a weaker field ligand reduces Δ_o . Based on this speculation, sulfides can be considered good candidates for exploring the existence of the HS/IS state of the Co³⁺ ion because the S²⁻ ion causes a weaker crystal field than the O²⁻ ion [9].

A suitable system for this purpose is Co₃S₄ (AB_2S_4 , $A = \text{Co}^{2+}$ and $B = \text{Co}^{3+}$). Spinel Co₃S₄ contains Co³⁺ ions at the octahedral site whose ground-state electron configuration is believed to be $t_{2g}^6 e_g^0$ (i.e., LS state, $S = 0$). The other Co species in Co₃S₄, the tetrahedral Co²⁺ ion, is known to have an electron configuration of $t_2^4 e^3$ (HS state, $S = 3/2$), similar to that of Co₃O₄. Hence, the transition from a paramagnetic (PM) to an antiferromagnetic (AFM) phase below the Néel temperature $T_N = 58$ K [10] was analyzed in terms of the exchange interactions between the tetrahedral HS Co²⁺ ions. However, the unexpected behavior of the octahedral Co³⁺ ions seems to induce atypical magnetic properties in the material. A few recent experiments have reported the ferromagnetic (FM) phases. For instance, Bao *et al.* [11] observed an FM phase whose stability strongly depends on the reaction time during the hydrothermal growth process. Liu *et al.* [12] measured the FM phase in the ultrathin Co₃S₄ nanosheets, and they suggested that the FM phase was induced by a combination of the LS \rightarrow HS transition of the octahedral Co³⁺ ion and Jahn-Teller distortion.

Furthermore, this material is potentially important from the aspect of exotic magnetism. This is because the spinel-structured AB_2X_4 ($X = \text{O}$ and S) systems exhibit exotic magnetic ground states (e.g., spin glass) owing to their unique and rather complex crystal symmetry [13]. The B sublattice forms a network of corner-sharing tetrahedra (pyrochlore

*minseokchoi.phd@gmail.com

lattice) that are comparable to geometrically frustrated magnets, and magnetic ions occupying the B sublattice induce fascinating magnetic states such as spin liquid and conical spiral states [14]. In addition, strong geometric frustration effects have been observed in exchange interactions on the A sublattice (diamond lattice) [15]. Indeed, exotic magnetic states are sought by substituting the other elements to the Co^{2+} site (e.g., CuCo_2S_4 [16]) or to the Co^{3+} site (e.g., CoAl_2S_4 [17]) in Co_3S_4 . $\text{Co}_3\text{Sn}_2\text{S}_2$ and related systems were also recently reported to be potential ferromagnetic (FM) Weyl semimetals [18], despite having a crystal structure that is different from spinel.

Therefore, octahedral Co ions need to be systematically investigated to properly understand the mechanisms leading to magnetism in Co_3S_4 as well as other cobalt compounds. In this study, we theoretically investigate the SCO behavior of the octahedral Co ion in Co_3S_4 to reveal the causes of its magnetic ambiguity and thereby discover hidden magnetic phases. Using the density-functional theory (DFT)+ U calculation, the experimentally known AFM phase was revisited, and then the hidden magnetic phases associated with the HS/IS Co^{3+} ion were explored. The obtained results are carefully compared with those of previous reports and are discussed in terms of the ligand field theory. Finally, the emergence of frustrated magnetism was examined.

II. REVISITING THE EXPERIMENTALLY REPORTED AFM PHASE

As listed in Table I, the calculated lattice constant and Co-S bond lengths of the AFM phase are larger than the experimental values ($a_0 = 9.406 \text{ \AA}$, $d_{\text{Co}^{2+}\text{-S}} = 2.18 \text{ \AA}$, $d_{\text{Co}^{3+}\text{-S}} = 2.27 \text{ \AA}$) [19] of the PM phase. The calculated values of the nonmagnetic metal phase ($a_0 = 9.323 \text{ \AA}$, $d_{\text{Co}^{2+}\text{-S}} = 2.15 \text{ \AA}$, $d_{\text{Co}^{3+}\text{-S}} = 2.26 \text{ \AA}$) are close to the experimental values of the PM phase, even though the calculation of the nonmagnetic state is a poor approximation of the PM state.

The spin direction of the two types of tetrahedral Co^{2+} [denoted as A and A' in Fig. 1(a)] alternated between up and down in the AFM phase. The Co^{2+} ions were in the HS state with a spin moment $\mu_{\text{Co}^{2+}}$ of $2.52\mu_B$. This was in agreement with the previously computed $\mu_{\text{Co}^{2+}}$ value, which is reported, in the relevant literature, to be in the range of theoretical values of $2.04\mu_B$ [20] and $2.55\mu_B$ [21]. However, it is considerably smaller than the experimental value of $3.26\mu_B$ for Co^{2+} in Co_3O_4 [22] (the experimental value for Co^{2+} in Co_3S_4 is unknown). The smaller value can be attributed to the strong covalency of the Co-S bond compared to the Co-O bond [23]. As expected, the Co^{3+} ions are found in the LS state, which is consistent with the previous studies reporting that Co^{3+} is nonmagnetic [20,21,24].

The critical temperature of the AFM to PM phase transition was estimated using the mean-field theory based on the Heisenberg Hamiltonian $H = -\sum_{A,A'} J_{AA'} \vec{S}_A \cdot \vec{S}_{A'}$, where $J_{AA'}$ denotes the exchange integral for the nearest neighbor A - A' interaction [25]. The spin magnitudes at the A (S_A) and A' ($S_{A'}$) sites were set to be $3/2$. Another FM configuration with parallel spin moments of A and A' was used which is energetically less stable than the AFM phase by 9.4 meV/f.u. , thereby resulting in a $J_{AA'}$ value of -0.626 meV . Consequently, the

TABLE I. Comparison of the calculated physical quantities of the AFM and FM phases: lattice constants (a_0 and c_0), Co-S bond lengths ($d_{\text{Co}^{2+}\text{-S}}$ and $d_{\text{Co}^{3+}\text{-S}}$), S-Co-S bond angle θ , Co spin magnetic moment μ , band gap energy E_g , the total energy difference between the AFM and FM phases ΔE_{tot} , and formation enthalpy ΔH^f . The space groups of all the phases are found using the default value (10^{-5}) of symmetry tolerance in the PHONOPY code. The lattice constants of the AFM phase are for the cubic conventional cell containing 56 atoms, and those of the FM phase are for a tetragonal conventional cell with 28 atoms. For comparison, the values of the FM phase in the representation of the pseudocubic cell are also noted in parentheses.

	AFM	FM
Space group	$Fd\bar{3}m$	$I4_1/amd$
a_0 (Å)	9.641	7.081(10.014)
c_0 (Å)		10.208 (10.208)
$d_{\text{Co}^{2+}\text{-S}}$ (Å)	2.312($\times 4$)	2.311 ($\times 4$)
$d_{\text{Co}^{3+}\text{-S}}$ (Å)	2.288 ($\times 6$)	2.441 ($\times 4$), 2.460 ($\times 2$)
$\theta_{\text{S-Co}^{2+}\text{-S}}$ (deg)	109.47	107.33, 110.55
$\theta_{\text{S-Co}^{3+}\text{-S}}$ (deg)	83.31, 96.69	86.86, 93.75
$\mu_{\text{Co}^{2+}}$ (μ_B)	2.52	2.52
$\mu_{\text{Co}^{3+}}$ (μ_B)	0	2.61 (mean)
E_g (eV)	0.91	0
ΔE_{tot} (eV/f.u.)		-1.31
ΔH^f (eV)	-5.40	-6.71

estimated critical temperature is 73 K, which is close to the experimental T_N of 58 K [10].

The AFM phase exhibits an indirect band gap [$E_g = 0.91 \text{ eV}$; Fig. 1(b)]. The value of E_g is comparable to the values of 0.5 eV obtained using $U_{\text{eff}} = 5$ and 0.7 eV obtained using $U_{\text{eff}} = 6.5 \text{ eV}$, respectively, in the previous Perdew-Burke-Ernzerhof functional + U study [21]. The conduction band minimum (CBM) was positioned at the X point, and the valence band maximum (VBM) was located at the (0.167, 0.167, 0.333) point along the K - Γ line (Σ_{max}). The positions of the valence band edge states at the Γ point and the (0.288, 0.288, 0.288) point along the Γ - L line (Λ_{max}) are close to the VBM. The energy difference between these edge states and the VBM is less than 0.1 eV. The optical gap (vertical) is estimated to be 1.56 eV at the CBM and 1.54 eV at the VBM. The conduction band and the valence band are mainly Co $3d$ -like and S $3p$ -like, respectively, indicating that the band gap opens between these states. Therefore, the electronic structure of the AFM phase corresponds to the charge-transfer type. Although the conduction band edges are characterized by Co $3d$ states, the effective masses of electrons ($0.565m_0$ along the $X \rightarrow \Gamma$ direction) are comparable to those in good electron conductors such as MoS_2 [26] (see Table 1 in Ref. [27]). The effective masses of the hole at the VBM Σ_{max} are $0.851m_0$ along the $\Sigma_{\text{max}} \rightarrow K$ point direction, which is comparable to those in p -type transparent oxides [28].

According to the Zaanen-Sawatzky-Allen model [29], the electronic structure of transition metal compounds can be understood in terms of the competition between U and Δ_{CT} , where U is the electron-electron on-site Coulomb repulsion energy and Δ_{CT} is the charge-transfer energy gap required for electron transfer from the ligand to the metal. When

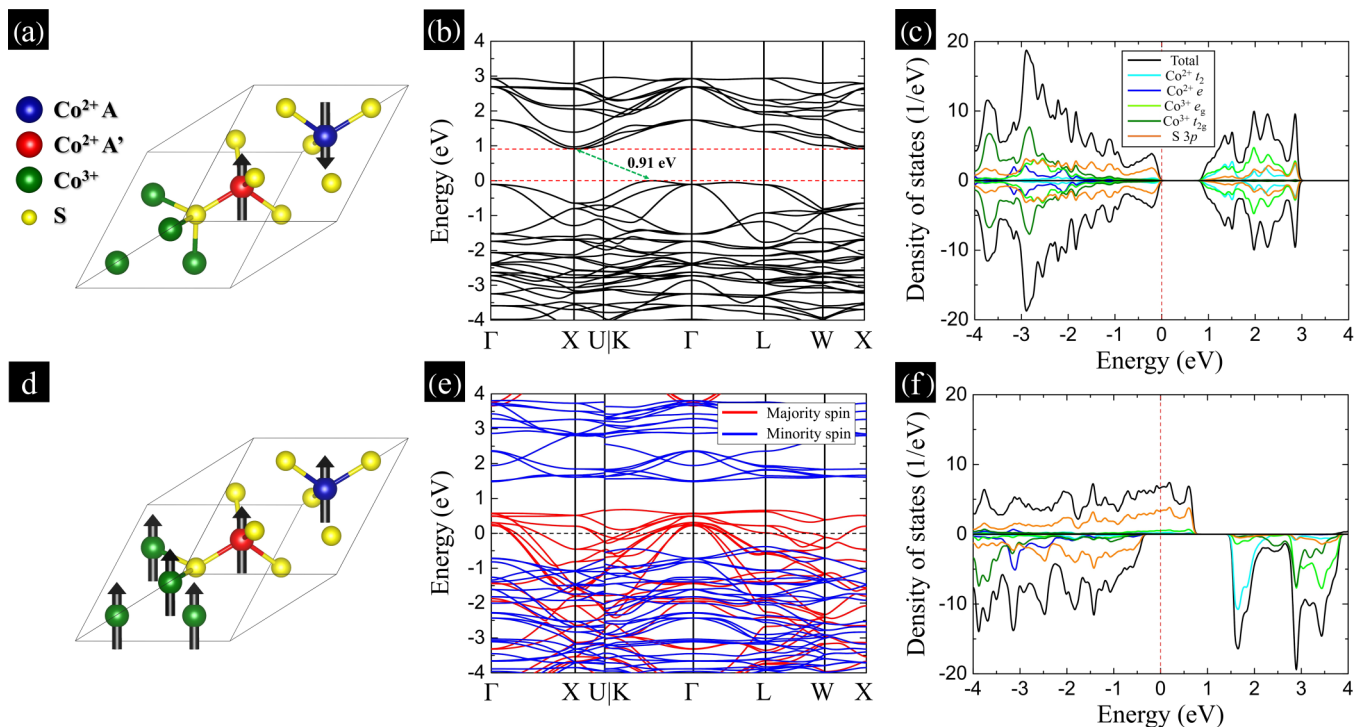


FIG. 1. Crystal structure, band structure, and density of states of (a)–(c) AFM and (d)–(f) FM Co_3S_4 . The high-symmetry k points are Γ $(0, 0, 0)$, X $(\frac{1}{2}, 0, \frac{1}{2})$, U $(\frac{5}{8}, \frac{1}{4}, \frac{5}{8})$, K $(\frac{3}{8}, \frac{3}{8}, \frac{3}{4})$, L $(\frac{1}{2}, \frac{1}{2}, \frac{1}{2})$, and W $(\frac{1}{2}, \frac{1}{4}, \frac{3}{4})$. For the density of states, total (black), $\text{Co}^{2+} t_2$ (cyan), $\text{Co}^{2+} e$ (blue), $\text{Co}^{3+} e_g$ (light green), $\text{Co}^{3+} t_{2g}$ (green), and S $3p$ (orange) states are illustrated. The highest electron-occupied state was set to zero.

$U < \Delta_{\text{CT}}$, a gap determined by the U energy opens between the fully occupied lower-energy d band and the unoccupied higher-energy d band. The insulator obtained as a result is Mott-Hubbard type. When $U > \Delta_{\text{CT}}$, a band gap appears which corresponds to the energy separation between the occupied ligand p band and the unoccupied d band, and the insulator obtained as a result is called the charge-transfer type. For Co_3S_4 , we evaluated U from the gap between the unoccupied and occupied Co $3d$ band centers and Δ_{CT} by the difference between the unoccupied Co $3d$ band center and the occupied S $3p$ band center [30]. The resulting values of U were 6.18 eV for $\text{Co}^{2+} 3d$ and 5.36 eV for $\text{Co}^{3+} 3d$, and that of Δ_{CT} is 4.98 eV. This indicates that $U > \Delta_{\text{CT}}$, indicating the charge-transfer picture as well.

Although the nonzero band gap observed in the AFM phase is consistent with the AFM insulating Co_3O_4 , the oxide counterpart of Co_3S_4 , it apparently disagrees with the experimentally obtained AFM metal phase. For example, Bouchard *et al.* reported the metallic characteristics of Co_3S_4 down to $T \sim 90$ K [31]; the nuclear magnetic resonance (NMR) measurements suggested that Co_3S_4 is a weak AFM metal with T_N of ~ 55 K [16]. Three plausible explanations exist for this discrepancy: (i) The homogeneous phase of Co_3S_4 is extremely difficult to achieve owing to the complicated stoichiometry of cobalt sulfides and the strong affinity of cobalt ions to oxygen [32]. Therefore, the secondary phase, which has a chemical composition different from Co_3S_4 , is likely to form in the Co_3S_4 specimens. Several NMR experiments previously suggested the presence of an FM half-metallic phase such as CoS_2 ($T_C = 124$ K) to explain anomalous magnetic behavior at

temperatures of ~ 60 K. [33,34], (ii) Analogous to explanation (i), moderate lattice defect formation occurs in Co_3S_4 . This can close the semiconducting gap and/or influence magnetic ordering. We observed that two kinds of Co vacancies and the S vacancy make the electronic structure of the AFM Co_3S_4 phase metallic (see Fig. 1 in Ref. [27]). (iii) The presence of the hidden phase cannot be excluded. As mentioned above, the FM phases were proposed by NMR experiments [33,34] and were observed in Refs. [11,12]. The following discussion focuses primarily on scenario (iii).

III. FM METAL PHASE PREDICTED THEORETICALLY

Our calculations show that the HS Co^{3+} is stabilized in Co_3S_4 by the enhancement of $\text{Co}^{3+} 3d$ –S $3p$ hybridization due to weak crystal-field splitting. Consequently, a different FM metal phase is obtained, and it is energetically more stable than the AFM phase by 1.31 eV/f.u. (Fig. 1 and Table I). Examining the U_{eff} dependence of the phase stability shows that U_{eff} values for Co^{3+} greater than ~ 5 eV consistently reproduce the results (see Fig. 2 in Ref. [27]).

Unlike the AFM phase, all the Co^{2+} and Co^{3+} ions in the FM metal phase are magnetically active, and their spin directions are parallel. The calculated $\mu_{\text{Co}^{3+}}$ was $2.61\mu_B$, which is close to the reported values of $2.88\mu_B$ – $3.11\mu_B$ for HS Co^{3+} ($t_{2g}^4 e_g^2$, $S = 2$) in LaCoO_3 [7,35]. The values of $\mu_{\text{Co}^{3+}}$ in Co_3S_4 being smaller than the ideal HS value for the $t_{2g}^4 e_g^2$ configuration can be attributed to strong Co $3d$ –S $3p$ hybridization. Moreover, this effect is more pronounced in sulfides than that in oxides, such as perovskite LaCoO_3 , because of the more

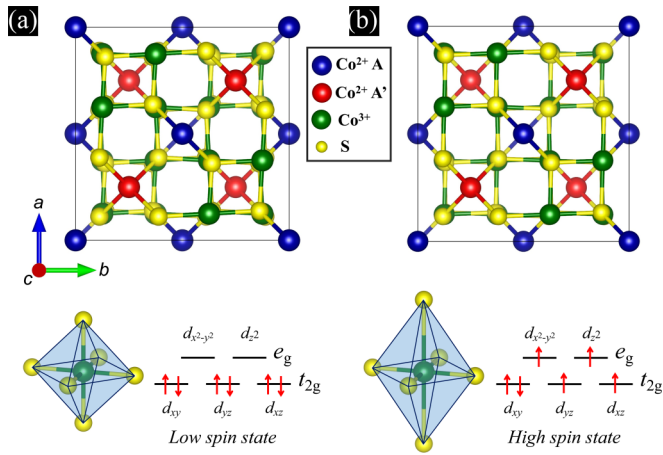


FIG. 2. Crystal structure of (a) AFM and (b) FM phases. In the AFM phase, the spin directions of Co^{2+} A and A' alternately repeat up and down, and the spin moment of Co^{3+} is zero. Nevertheless, the spin directions of Co^{2+} A and A' are parallel, and the mean spin moment of Co^{3+} is $2.61\mu_B$ in the FM phase.

covalent character of Co-S bonds in comparison to Co-O bonds [23]. However, it is noteworthy that according to the literature, DFT+ U approaches have reproduced IS Co^{3+} ($t_{2g}^5 e_g^1$, $S = 1$) with spin moments close to the ideal value of $2\mu_B$ [7,35,36]. We also found a similar magnetic phase involving $\mu_{\text{Co}^{3+}} = 1.9\mu_B$, possibly IS Co^{3+} , but it is less stable than that of the HS Co^{3+} FM phase by 2.05 eV/f.u.

The lattice constants and $d_{\text{Co}^{3+}-\text{S}}$ in the FM phase are considerably larger than those in the AFM phase, which is consistent with the increase in the ionic radius of Co^{3+} from 0.69 Å in the LS state to 0.75 Å in the HS state [37]. Interestingly, two $d_{\text{Co}^{3+}-\text{S}}$ for the bonds along the c axis become slightly longer than the other four bonds, whereas $d_{\text{Co}^{2+}-\text{S}}$ in both phases are almost identical. This change in the Co^{3+} spin state makes the distorted cuboid comprising Co^{3+} and O^{2-} in the spinel structure straighter, resulting in tetragonal symmetry (Fig. 2).

The FM phase is half metallic, where the electronic structure has an energy gap of over 2 eV in the minority-spin channel [Figs. 1(e) and 1(f)]. This is consistent with the unknown phase proposed by the NMR experiments [33,34]. The valence band primarily comprises S 3*p* in the majority channel, and the conduction band is predominantly characterized by Co^{2+} t_2 in the minority channel. The density of states profiles for Co^{2+} 3*d* states are not dramatically changed, which is consistent with the identical $d_{\text{Co}^{2+}-\text{S}}$ in the AFM and FM phases [Figs. 3(a) and 3(b)]. In contrast, significant changes in the Co^{3+} 3*d* states are observed, as expected. The elongation along the c axis splits the triply degenerate t_{2g} states to doubly degenerate lower-energy states (d_{yz} , d_{xz}) and a single higher-energy state (d_{xy}) and splits the e_g states into a higher $d_{x^2-y^2}$ and lower d_{z^2} [Figs. 3(c) and 3(d)]. However, the difference in length between the elongated bonds and the rest is quite small (~ 0.02 Å). Conversely, in the FM Co_3S_4 nanosheets [12], elongation along the cubic c axis and compression along the other two directions occur simultaneously.

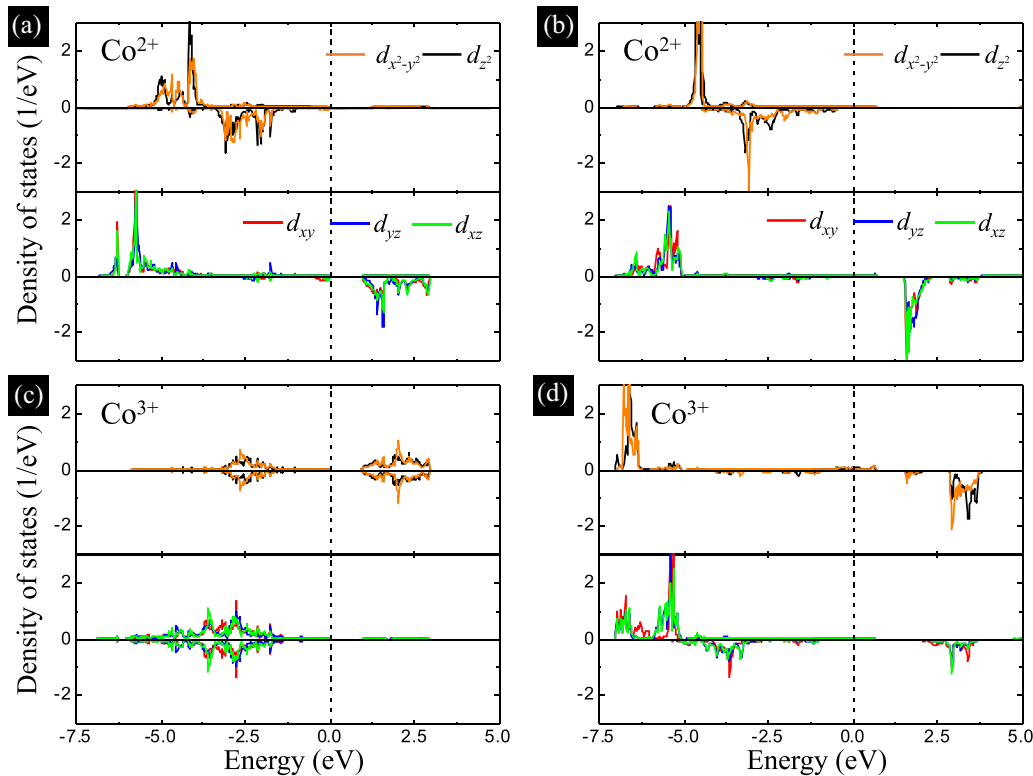


FIG. 3. Partial density of states for Co^{2+} 3*d* and Co^{3+} 3*d* states in the (a) and (c) AFM and (b) and (d) FM phases. The highest electron occupied state was set to zero.

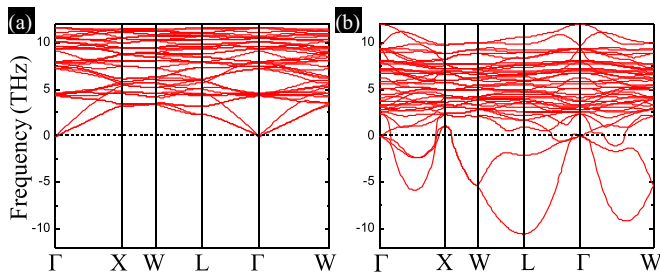


FIG. 4. Phonon band structures of (a) AFM and (b) FM phases. The negative value of the frequency is responsible for the imaginary mode.

The dynamical stability of the AFM and FM phases was examined by studying their phonon spectra (Fig. 4). The presence of imaginary frequencies in the phonon spectra of a material indicates that the material is dynamically unstable and can undergo phase transitions to find a dynamically stable phase. The AFM phase was found to be dynamically stable since there are no imaginary frequencies (i.e., no negative frequencies) in the phonon spectrum. This agrees with the belief that this phase is the magnetic ground state of Co_3S_4 , similar to Co_3O_4 . Although small imaginary frequencies ($1\text{--}2\text{ cm}^{-1}$) are observed near the Γ point, such a small instability is likely to be illusory owing to the numerical errors in the calculations [38,39]. In contrast, the FM phase was found to be dynamically unstable since it clearly exhibits imaginary frequencies, indicating the existence of further phase transition from the FM phase, which will be discussed in the last section. An important point is that although the FM phase is dynamically unstable, it is energetically more stable than the AFM phase. Therefore, we suggest that the experimentally measured AFM phase is the ground state of cubic spinel Co_3S_4 and the predicted FM phase is another stable polymorph involving the HS Co^{3+} .

According to our calculations, the predicted FM metal phase is expected to appear under appropriate chemical, thermal, or mechanical experimental conditions. The condition under which tensile strain/pressure is applied to the Co_3S_4 sample is assumed to be one possible case. The high-spin Co^{3+} extends the bond length of the Co-S bond, so the FM phase exhibits a much larger cell volume than the AFM phase. Indeed, we found that the FM phase is always more stable than the AFM phase and becomes more stable with increasing cell volume (see Fig. 3 in Ref. [27]). This means that if the Co_3S_4 sample in experiment is volume expanded, the FM phase may appear.

Furthermore, ferrimagnetic (FiM), and other AFM (AFM-II) phases, involving the HS Co^{3+} , were found (see Fig. 4 and Table 2 in Ref. [27]). These are more stable than the experimentally reported AFM phase (by 1.30 eV/f.u. for FiM and 1.19 eV/f.u. for AFM-II). In terms of energetics, the phase stability is in the following order: $\text{FM} > \text{FiM} > \text{AFM-II} > \text{AFM}$. The FiM ($\mu_{\text{Co}^{3+}} \sim 2.57\mu_{\text{B}}$) and AFM-II ($\mu_{\text{Co}^{3+}} \sim 2.57\mu_{\text{B}}$) phases crystalize into the tetragonal structure, similar to the FM phase.

In the FiM phase, the spin orientations of Co^{2+} A and A' are antiparallel, whereas the Co^{3+} spins are parallel. In contrast,

the Néel FiM configuration has an array of antiparallel Co^{2+} and Co^{3+} spins, similar to CoCr_2S_4 ($T_C = 222\text{ K}$) where Cr^{3+} ($S = 3/2$) replaces Co^{3+} [40]. However, it is found to be slightly less stable than the FiM phase (by 0.03 eV/f.u.). The electronic structure of the FiM phase is similar to that of the FM phase. A significant difference is the existence of narrow Co^{2+} t_2 -like states in the FiM phase, at $\sim 1\text{ eV}$ above the valence band in the majority-spin channel. The AFM-II phase is also metallic; its magnetism originates from the AFM exchange interaction of $\text{Co}^{2+} - \text{Co}^{2+}$, $\text{Co}^{2+} - \text{Co}^{3+}$, and $\text{Co}^{3+} - \text{Co}^{3+}$. The conduction band apparently comprises two narrow d bands. The lower band is Co^{2+} t_2 -like, and the upper band is Co^{3+} t_{2g} and e_g -like. The valence band primarily comprises S $3p$, similar to the AFM.

IV. FORMATION OF HS Co^{3+} AND WEAK JAHN-TELLER-LIKE ELONGATION

As mentioned above, our DFT+ U results indicate that the HS Co^{3+} can be obtained, which results in the FM metal phase. The ligand-field theory justifies these results. According to the theory, the crystal-field stabilization energy (CFSE) determines which configuration of the d electron is energetically likely for each element and oxidation state, depending on the metal-ligand environment. The CFSE for Co^{3+} at the octahedral site is $-\frac{2}{5}\Delta_o$ for the HS state ($t_{2g}^4 e_g^2$) and $-\frac{12}{5}\Delta_o + P$ for the LS state ($t_{2g}^6 e_g^0$), where Δ_o and P are the crystal-field splitting energy at the octahedral site and spin pairing energy, respectively [37]. Δ_o is estimated to be 1.80 eV for Co_3O_4 [41], and P for Co^{3+} is 2.60 eV [37]. Thus, CFSE for HS Co^{3+} (-0.72 eV) $>$ CFSE for LS Co^{3+} (-1.72 eV), resulting in the stabilization of LS Co^{3+} at the octahedra site in Co_3O_4 . For Co_3S_4 , the magnitude of Δ_o should be smaller because the S^{2-} causes a weaker crystal field than the O^{2-} [9]. Here, we assume Δ_o is 0.66 eV in Co_3S_4 by roughly estimating a ratio between Δ_o of 1.05 eV for CoO and 0.4 eV for CoS [42] (Δ_o in Co_3S_4 is unknown). Consequently, the estimated CFSE is -0.264 eV (HS, $S = 2$) $<$ $+1.02\text{ eV}$ (LS, $S = 0$), enabling the formation of HS Co^{3+} in Co_3S_4 .

The weak Jahn-Teller-like elongation further stabilizes the HS Co^{3+} formation. Using the ionic crystal-field parameters and the hybridization strengths estimated according to Harrison's description, Agrestini *et al.* [43] demonstrated that when the in-plane Co-O distance is enlarged, the HS Co^{3+} remains in the ground state regardless of the tetragonal elongation of the CoO octahedra. Both a lengthened out-of-plane Co-O distance and a shortened in-plane Co-O distance are required to form an IS Co^{3+} . The predicted FM Co_3S_4 satisfies this HS condition. Both the out-of-plane and in-plane $d_{\text{Co}^{3+}-\text{S}}$ are enlarged by $\sim 7\%$ compared to the AFM phase. Moreover, the out-of-plane $d_{\text{Co}^{3+}-\text{S}}$ is $\sim 0.02\text{ \AA}$ longer than the in-plane $d_{\text{Co}^{3+}-\text{S}}$. Therefore, the HS state is more likely to form in the FM metal phase compared to the IS or LS states. In addition, we used the DFT+ U calculation to analyze how the bond elongation affects the stabilization of the HS state and the FM phase. In this analysis, we evaluated the differences in total energy and magnetic properties with and without the bond elongation using the lattice of the AFM phase. Our results show that despite a small bond elongation ($\sim 0.01\text{ \AA}$) along

the c axis, the total energy gains 0.5 eV/f.u., accompanied by a $\mu_{\text{Co}^{3+}}$ of $2.51\mu_B$.

V. POSSIBILITY OF THE EMERGENCE OF FRUSTRATED MAGNETISM

Exotic magnetic ground states have been widely observed in magnetic spinel compounds [13]. Therefore, we discuss the possibility of a phase transition from the predicted FM phase to the frustrated magnetic state in Co_3S_4 . Similar exotic ground states are expected in Co_3S_4 because its structure is similar to that of spinel, and its FM phase is dynamically unstable (Fig. 4), which implies the possibility of the existence of further phase transitions.

The frustration strength is often estimated using the frustration parameter $f = |\Theta_{\text{CW}}|/T_C$ or T_N , where Θ_{CW} is the Curie-Weiss temperature. When $f = 1$, nominal long-range ordering leads to the ground state, whereas when $f > 1$, the possibility of the appearance of frustrated magnetism cannot be excluded. For example, the f parameter of Co_3O_4 , the oxide counterpart of Co_3S_4 , is 3.9 [44]. This triggers extensive investigation of frustrated magnetism in the oxide by substituting several elements to the Co sites [13]. CoCr_2O_4 , in which the Co^{3+} sites are replaced by magnetic Cr, exhibited a conical magnetic ground state with $T_N = 25$ K, and CoAl_2O_4 , in which Al ions replace the Co^{3+} ions, exhibited spin-glass behavior with $T_N = 4.8$ K [44]. The f parameter of the frustrated systems is 6.99 for CoCr_2O_4 and 19 for CoAl_2O_4 [13].

Although the f parameter for Co_3S_4 is unclear, the possibility of magnetic frustration in the material cannot be ruled out: it is either 1 [34] or 5 [16], depending on the temperature range for the fitting procedure to extract Θ_{CW} . Several efforts have been made to find frustrated magnetism in Co_3S_4 -based systems. For instance, the magnetic Cu doped at the Co^{2+} site in Co_3S_4 , i.e., $(\text{Co}_{1-x}\text{Cu}_x)\text{Co}_2\text{S}_4$, reveals the superconducting state, but no frustrated magnetism was observed [16,34]. CoCr_2S_4 , the counterpart of CoCr_2O_4 , is a FiM insulator with $T_N = 222$ K [40]. CoAl_2S_4 exhibits a frustrated AFM phase (spin-glass-like behavior at $T \sim 5$ K) with $f = 46$, although its crystal structure resembles that of FeGa_2S_4 type [17].

In addition to the f parameter, the emergence of geometrical frustration in cubic spinel can be examined using the parameter $u = (4J_{\text{BB}}S_{\text{B}})/(3J_{\text{AB}}S_{\text{A}})$, as proposed by Lyons, Kaplan,

Dwight, and Menyuk (LKDM) [45,46]. Here, J_{BB} and J_{AB} denote the exchange constants for the nearest neighbor B - B and A - B interactions, respectively, and S_{A} and S_{B} are the spin magnitudes at the A and B sites, respectively. The LKDM theory, which is based on the Heisenberg Hamiltonian, provides the ground state of cubic spinel in terms of the competition between the nearest neighbor B - B and A - B exchange interactions, while exchange interactions between A - A sites are ignored. When $u < 8/9$, the Néel configuration is the ground state, where all the A -site spins are mutually parallel and antiparallel to all the B -site spins. When $8/9 < u < 1.298$, the spin conical state is stable. When $u > 1.298$, the spin conical state is suppressed. We applied the LKDM theory to Co_3S_4 by evaluating the parameter u and J values for Co_3S_4 (see Ref. [27] for details). J_{AA} was also calculated because the nearest neighbor AFM A - A interaction enhances frustration and thereby suppresses the conical spin order [47]. S_{A} and S_{B} were set to $3/2$ and $4/2$, respectively. Our results show that $u = 8.450$ with $J_{\text{AA}} = -0.710$ meV, $J_{\text{BB}} = 1.922$ meV, and $J_{\text{AB}} = 0.384$ meV, indicating that geometrical magnetic frustration may appear from the FM phase when the temperature is lowered.

In summary, through first-principles DFT+ U approaches and ligand-field theory, we predicted the stabilization of the HS state of the octahedral Co^{3+} ion in Co_3S_4 as well as the related magnetic phases. The HS state of the Co^{3+} ion is likely to form along with a weak Jahn-Teller-like elongation. This leads to the stabilization of an FM metal phase that is energetically more stable than the experimentally known AFM phase but is dynamically unstable. Furthermore, by applying the LKDM theory, additional phase transitions from the FM metal phase to the frustrated magnetic phase are predicted. Our findings provide insight into magnetism in cobalt spinels and encourage further investigation of the hidden magnetic states of the sulfides.

ACKNOWLEDGMENTS

We thank Hyungjeon Jeon and Seung Soo Oh for their constructive discussions and helpful comments. This research was supported by the Basic Science Research Program through the National Research Foundation of Korea (NRF) funded by the Ministry of Education (Grant No. NRF-2021R1F1A1051716).

-
- [1] P. Gütllich and H. A. Goodwin, Spin crossover—An overall perspective, in *Spin Crossover in Transition Metal Compounds I*, edited by P. Gütllich and H. Goodwin (Springer, Berlin, Heidelberg, 2004), pp. 1–47.
- [2] T. Kitazawa, Synthesis and applications of new spin crossover compounds, *Crystals* **9**, 382 (2019).
- [3] M. Meng, Y. Sun, Y. Li, Q. An, Z. Wang, Z. Lin, F. Yang, X. Zhu, P. Gao, and J. Guo, Three dimensional band-filling control of complex oxides triggered by interfacial electron transfer, *Nat. Commun.* **12**, 2447 (2021).
- [4] R. Schmidt, J. Wu, C. Leighton, and I. Terry, Dielectric response to the low-temperature magnetic defect structure and spin state transition in polycrystalline LaCoO_3 , *Phys. Rev. B* **79**, 125105 (2009).
- [5] M. A. Señarís-Rodríguez and J. B. Goodenough, LaCoO_3 revisited, *J. Solid State Chem.* **116**, 224 (1995).
- [6] C. N. R. Rao, M. M. Seikh, and C. Narayana, Spin-state transition in LaCoO_3 and related materials, in *Spin Crossover in Transition Metal Compounds II* (Springer, Berlin, 2004), pp. 1–21.
- [7] M. A. Korotin, S. Y. Ezhov, I. V. Solovyev, V. I. Anisimov, D. I. Khomskii, and G. A. Sawatzky, Intermediate-spin state and properties of LaCoO_3 , *Phys. Rev. B* **54**, 5309 (1996).

- [8] M. Kagan, K. Kugel, and A. Rakhmanov, Electronic phase separation: Recent progress in the old problem, *Phys. Rep.* **916**, 1 (2021).
- [9] P. Bajpai, *NEET 2020 Chemistry Guide*, 7th ed. (Disha Publication, New Delhi, 2019).
- [10] H. Nishihara, T. Kanomata, T. Kaneko, and H. Yasuoka, Pulsed nuclear magnetic resonance of ^{59}Co in Co_3S_4 , *J. Appl. Phys.* **69**, 4618 (1991).
- [11] S.-J. Bao, Y. Li, C. M. Li, Q. Bao, Q. Lu, and J. Guo, Shape evolution and magnetic properties of cobalt sulfide, *Cryst. Growth Des.* **8**, 3745 (2008).
- [12] Y. Liu, C. Xiao, M. Lyu, Y. Lin, W. Cai, P. Huang, W. Tong, Y. Zou, and Y. Xie, Ultrathin Co_3S_4 nanosheets that synergistically engineer spin states and exposed polyhedra that promote water oxidation under neutral conditions, *Angew. Chem. Int. Ed.* **54**, 11231 (2015).
- [13] H. Takagi and S. Niitaka, Highly frustrated magnetism in spinels, in *Introduction to Frustrated Magnetism: Materials, Experiments, Theory*, edited by C. Lacroix, P. Mendels, and F. Mila (Springer, Berlin, 2011), pp. 155–175.
- [14] S.-H. Lee, H. Takagi, D. Louca, M. Matsuda, S. Ji, H. Ueda, Y. Ueda, T. Katsufuji, J.-H. Chung, S. Park, S.-W. Cheong, and C. Broholm, Frustrated magnetism and cooperative phase transitions in spinels, *J. Phys. Soc. Jpn.* **79**, 011004 (2010).
- [15] V. Fritsch, J. Hemberger, N. Büttgen, E.-W. Scheidt, H.-A. Krug von Nidda, A. Loidl, and V. Tsurkan, Spin and Orbital Frustration in MnSc_2S_4 and FeSc_2S_4 , *Phys. Rev. Lett.* **92**, 116401 (2004).
- [16] H. Sugita, S. Wada, Y. Yamada, K. Miyatani, and T. Tanaka, NMR investigation of an itinerant weakly antiferromagnetism in metallic thiospinels CoCo_2S_2 and $(\text{Co}_{1-x}\text{Cu}_x)\text{Co}_2\text{S}_4$, *J. Phys. Soc. Jpn.* **67**, 1401 (1998).
- [17] M. C. Menard, R. Ishii, T. Higo, E. Nishibori, H. Sawa, S. Nakatsuji, and J. Y. Chan, High-resolution synchrotron studies and magnetic properties of frustrated antiferromagnets MAl_2S_4 ($M = \text{Mn}^{2+}$, Fe^{2+} , Co^{2+}), *Chem. Mater.* **23**, 3086 (2011).
- [18] E. Liu *et al.*, Giant anomalous Hall effect in a ferromagnetic kagome-lattice semimetal, *Nat. Phys.* **14**, 1125 (2018).
- [19] O. Knop, K. I. G. Reid, Sutarno, and Y. Nakagawa, Chalkogenides of the transition elements. VI. x-ray, neutron, and magnetic investigation of the spinels Co_3O_4 , NiCo_2O_4 , Co_3S_4 , and NiCo_2S_4 , *Can. J. Chem.* **46**, 3463 (1968).
- [20] R. Z. Wang and Y. Zhang, Magnetism modulation of Co_3S_4 towards the efficient hydrogen evolution reaction, *Mol. Syst. Des. Eng.* **5**, 565 (2020).
- [21] R. Samal, S. Mondal, A. S. Gangan, B. Chakraborty, and C. S. Rout, Comparative electrochemical energy storage performance of cobalt sulfide and cobalt oxide nanosheets: Experimental and theoretical insights from density functional theory simulations, *Phys. Chem. Chem. Phys.* **22**, 7903 (2020).
- [22] W. Roth, The magnetic structure of Co_3O_4 , *J. Phys. Chem. Solids* **25**, 1 (1964).
- [23] D. Santos-Carballal, A. Roldan, R. Grau-Crespo, and N. H. de Leeuw, First-principles study of the inversion thermodynamics and electronic structure of FeM_2X_4 (thio)spinels ($M = \text{Cr}$, Mn , Co , Ni ; $X = \text{O}$, S), *Phys. Rev. B* **91**, 195106 (2015).
- [24] I. Kim, H.-H. Nahm, and M. Choi, First-principles study of antiferromagnetic cobalt spinels, *Curr. Appl. Phys.* **22**, 65 (2021).
- [25] A. Broese van Groenou, P. Bongers, and A. Stuyts, Magnetism, microstructure and crystal chemistry of spinel ferrites, *Mater. Sci. Eng.* **3**, 317 (1969).
- [26] H. Peelaers and C. G. Van de Walle, Effects of strain on band structure and effective masses in MoS_2 , *Phys. Rev. B* **86**, 241401(R) (2012).
- [27] See Supplemental Material at <http://link.aps.org/supplemental/10.1103/PhysRevResearch.4.033171> for details on the computational method, electronic and crystal structures of metastable phases, effective masses, and calculations of exchange parameters.
- [28] G. Hautier, A. Miglio, G. Ceder, G.-M. Rignanese, and X. Gonze, Identification and design principles of low hole effective mass p-type transparent conducting oxides, *Nat. Commun.* **4**, 2292 (2013).
- [29] J. Zaanen, G. A. Sawatzky, and J. W. Allen, Band Gaps and Electronic Structure of Transition-Metal Compounds, *Phys. Rev. Lett.* **55**, 418 (1985).
- [30] I. Kim, J. Do, H. Kim, and Y. Jung, Charge-transfer descriptor for the cycle performance of $\beta\text{-Li}_2\text{MO}_3$ cathodes: Role of oxygen dimers, *J. Mater. Chem. A* **8**, 2663 (2020).
- [31] R. J. Bouchard, P. A. Russo, and A. Wold, Preparation and electrical properties of some thiospinels, *Inorg. Chem.* **4**, 685 (1965).
- [32] Q. Liu and J. Zhang, A general and controllable synthesis of Co_mS_n (Co_9S_8 , Co_3S_4 , and Co_{1-x}S) hierarchical microspheres with homogeneous phases, *CrystEngComm* **15**, 5087 (2013).
- [33] H. Saji and T. Yamadaya, Nuclear magnetic resonance (NMR) study of Co^{3+} in Co_3S_4 , *Phys. Lett. A* **41**, 365 (1972).
- [34] S. Wada, H. Sugita, K. Miyatani, T. Tanaka, and T. Nishikawa, Weak antiferromagnetism and superconductivity in pseudobinary spinel compounds $(\text{Cu},\text{Co})\text{Co}_2\text{S}_4$ investigated by ^{59}Co and ^{63}Cu magnetic resonance, *J. Phys.: Condens. Matter* **14**, 219 (2002).
- [35] A. M. Ritzmann, M. Pavone, A. B. Munoz-Garcia, J. A. Keith, and E. A. Carter, Ab initio DFT+U analysis of oxygen transport in LaCoO_3 : The effect of Co^{3+} magnetic states, *J. Mater. Chem. A* **2**, 8060 (2014).
- [36] K. Knížek, P. Novák, and Z. Jirák, Spin state of LaCoO_3 : Dependence on CoO_6 octahedra geometry, *Phys. Rev. B* **71**, 054420 (2005).
- [37] G. L. Miessler and D. A. Tarr, *Inorganic Chemistry*, 3rd ed. (Prentice Hall, New Jersey, 2004).
- [38] Y. Wang and J. Ren, Computational discovery of two-dimensional HfO_2 zoo based on evolutionary structure search, *Phys. Chem. Chem. Phys.* **22**, 4481 (2020).
- [39] I. Kim, G. Lee, and M. Choi, First-principles investigation of two-dimensional 1T-TiO_2 , *Phys. Rev. Mater.* **4**, 094001 (2020).
- [40] V. Felea, P. T. Cong, L. Prodan, Y. Gritsenko, J. Wosnitza, S. Zherlitsyn, and V. Tsurkan, Magnetic and acoustic properties of CoCr_2S_4 , *Low Temp. Phys.* **43**, 1290 (2017).
- [41] A. M. Hibberd, H. Q. Doan, E. N. Glass, F. M. F. de Groot, C. L. Hill, and T. Cuk, Co polyoxometalates and a Co_3O_4 thin film investigated by l-edge x-ray absorption spectroscopy, *J. Phys. Chem. C* **119**, 4173 (2015).
- [42] M. Al Samarai, M. U. Delgado-Jaime, H. Ishii, N. Hiraoka, K.-D. Tsuei, J. Rueff, B. Lassale-Kaiser, B. M. Weckhuysen, and F. M. de Groot, $1s3p$ resonant inelastic x-ray scattering of cobalt oxides and sulfides, *J. Phys. Chem. C* **120**, 24063 (2016).

- [43] S. Agrestini, C.-Y. Kuo, D. Mikhailova, K. Chen, P. Ohresser, T. W. Pi, H. Guo, A. C. Komarek, A. Tanaka, Z. Hu, and L. H. Tjeng, Intricacies of the Co^{3+} spin state in $\text{Sr}_2\text{Co}_{0.5}\text{Ir}_{0.5}\text{O}_4$: An x-ray absorption and magnetic circular dichroism study, *Phys. Rev. B* **95**, 245131 (2017).
- [44] N. Tristan, J. Hemberger, A. Krimmel, H.-A. Krug von Nidda, V. Tsurkan, and A. Loidl, Geometric frustration in the cubic spinels $M\text{Al}_2\text{O}_4$ ($M = \text{Co}, \text{Fe}, \text{and Mn}$), *Phys. Rev. B* **72**, 174404 (2005).
- [45] T. A. Kaplan, K. Dwight, D. Lyons, and N. Menyuk, Classical theory of the ground spin state in spinels, *J. Appl. Phys.* **32**, S13 (1961).
- [46] D. H. Lyons, T. A. Kaplan, K. Dwight, and N. Menyuk, Classical theory of the ground spin-state in cubic spinels, *Phys. Rev.* **126**, 540 (1962).
- [47] X. Yao, Stable and locally stable conditions for a conical spin state in the spinel structure, *Europhys. Lett.* **102**, 67013 (2013).